

# Assessment of Interslice MT Signal Characteristics of bSSFP for MTR Imaging of the Human Brain

Jeffrey William Barker<sup>1,2</sup>, Kyongtae Ty Bae<sup>1</sup>, and Sung-Hong Park<sup>1,3</sup>

<sup>1</sup>Radiology, University of Pittsburgh, Pittsburgh, Pennsylvania, United States, <sup>2</sup>Bioengineering, University of Pittsburgh, Pittsburgh, Pennsylvania, United States, <sup>3</sup>Bio and Brain Engineering, Korean Advanced Institute of Science and Technology, Daejeon, Yuseong-gu, Korea

**Purpose:** To assess the signal characteristics of interslice magnetization transfer (MT) effects of balanced steady state free precession (bSSFP) for interslice magnetization transfer ratio (MTR) imaging of the brain.

**Introduction:** Previously, interslice MT effects have been utilized for MT asymmetry imaging with the balanced steady-state free precession (bSSFP) sequence [1]. This method generates MT contrast without the need for a separate saturation pulse. Extension of this concept to MTR imaging is easily accomplished by acquiring an additional set of non-MT weighted reference images by adding an interslice delay sufficient for  $T_1$  recovery. Thus, MTR can be calculated pixel by pixel as  $MTR = 100\% \times (S_{MT} - S_{Ref}) / S_{Ref}$ , in which  $S_{MT}$  and  $S_{Ref}$  are the signal intensities of corresponding pixels in the MT-weighted and reference images, respectively. In this work, we acquired interslice MTR images in the brain of healthy normal subjects (N=6, age 24-39) for varying flip angle and phase encoding (PE) order. We also compared *in vivo* MTR values to two-pool model [2] simulations.

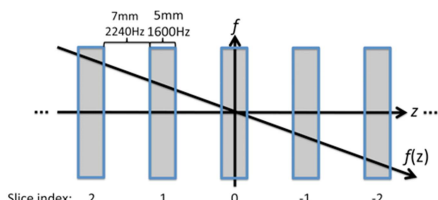


**Figure 1.** The application of a gradient varies the spin frequencies  $f(z)$  linearly in space ( $z$ ). Excitation of slice 0 will give off-resonance irradiation at respective frequency offsets of 3840Hz and 7680Hz to future slices 1 and 2.

**Theory:** Application of a slice-select gradient causes spatially varying spin frequencies. Excitation of a slice of interest is achieved by adjusting RF-pulse frequency. The slice of interest receives on-resonance excitation; however, the rest of the volume receives off-resonance irradiation. Excitation pulses during acquisition of one slice are effectively a train of off-resonance saturation pulses to future slices (Fig. 1). The off-resonance frequency received by neighboring slices is given by  $\delta_n = BW \cdot (1 + GAP/THK) \cdot n \cdot \text{sign}(GRAD) \cdot ORD$ , in which  $BW$  is the bandwidth of the RF-pulse,  $GAP$  is the interslice gap;  $THK$  is the slice thickness;  $n$  is the slice index with positive indices indicating future slices;  $\text{sign}(GRAD)$  is the sign of the gradient;  $ORD$  is +1 if ascending slice order and -1 if descending slice order.

Magnetization transfer effects can be modeled with two pools of protons: free water protons and macromolecular protons [2]. Macromolecular protons, which cannot be imaged directly due to fast transverse relaxation ( $T_2 \sim 10\mu s$ ), have a very broad absorption lineshape and are preferentially saturated by off-resonance RF irradiation. This saturation is then transferred to the free water pool via exchange of longitudinal magnetization. The system is mathematically modeled by modified Bloch equations that include terms for exchange and saturation [2].

**Methods:** All imaging experiments were approved by the Institutional Review Board and performed on a Siemens 3T Trio system (Siemens Medical Solutions, Erlangen, Germany). A 12-element head matrix coil was used for all data acquisitions.

MTR images were acquired at varying flip angle from  $15^\circ$  to  $90^\circ$  at  $15^\circ$  intervals. Scan parameters were: descending slice order; negative slice-select gradient; positive readout gradient; TR/TE = 4.11/2.06ms; matrix size =  $128 \times 128$ ; field of view =  $230 \times 230 \text{mm}^2$ ; slice thickness = 5mm; interslice gap = 7mm; scan direction = axial; PE direction = anterior-posterior; initial dummy PE steps = 10/30 for linear/centric PE order; phase oversampling = 50%; number of averages = 1; RF-pulse BW = 1100Hz; acquisition BW = 673Hz/pixel; number of slices = 15 for MT-weighted images (including dummy slices) and 7 for reference images; interslice delay = 0s for MT-weighted images and 8s for reference images. Scan time for MT-weighted images and reference images was 13s and ~1min, respectively. We also measured the observed  $T_2$  value of the center brain slice using a multi-contrast spin echo sequence. Regions of interest (ROI) located in the corpus callosum white matter (WM) and frontal gray matter (GM) of the center slice were used to calculate mean MTR values as a function of flip angle and PE order.

Simulations of the two-pool model from Ref. [2] were performed using the MT parameters from Ref. [3] for GM and WM. We considered five prior slices of off-resonance saturation (e.g., 13200Hz, 10560Hz, 7920Hz, 5280Hz, 2640Hz) for MT-weighting. For reference image signal, the acquisition slice was simulated with no prior slices of off-resonance saturation. Simulation parameters were taken to match acquisition parameters, such as flip angle, PE steps, repetition time (TR), and RF duration. Equations 1-4 were solved using the 4th/5th order Runge-Kutta algorithm. For analysis, we calculated MTR values using the magnitude of the transverse magnetization at the center line of k-space.

**Results and Discussion:** Figure 2a shows representative center slice images for varying flip angle and for linear and centric PE. Centric PE images showed better GM and WM contrast, suggesting that linear PE image contrast was influenced by relaxation effects. Figures 3b and 3c show the results of the ROI analysis and two-pool model simulations. Overall, MTR and SNR values increased with flip angle within the tested range. Centric PE images showed higher MTR values and substantially higher SNR than linear PE images (Figure 3d). Simulated MTR values agreed well with the *in vivo* measurements. Simulated MTR values for WM were 30-50% less than *in vivo* measurements for linear PE (data not shown) at high flip angles  $60^\circ$ - $90^\circ$ ; however, substitution of the observed  $T_2$  value of 85ms for the literature value (69ms,[3]) produced simulated MTR values in close agreement with *in vivo* results. We attribute this result to partial volume effects of cerebrospinal fluid.

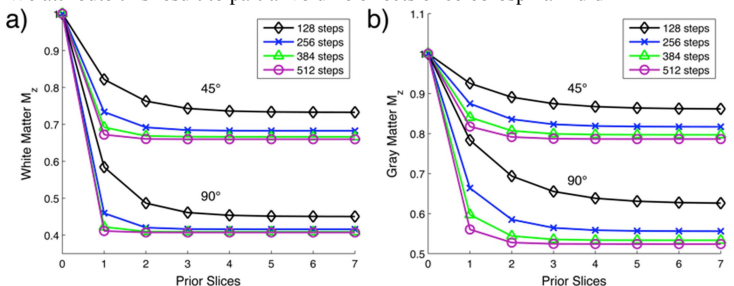


**Figure 3.** Simulations of longitudinal magnetization as a function of prior slices, PE steps per slice, flip angle, and for gray (a) and white (b) matter.

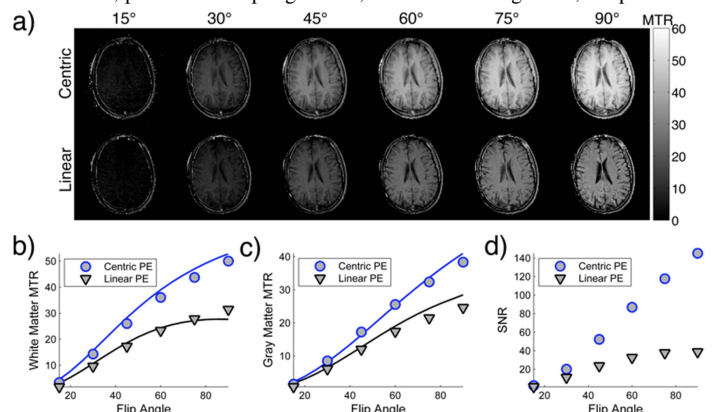


**Figure 2. a:** MTR images from a representative subject. Mean MTR values across subjects from ROI analysis for WM (b) and GM (c) are shown. The standard deviation across subjects was less than 2% MTR units for all data points. Simulated MTR values (solid lines) agreed well with *in vivo* data. d: SNR as function of flip angle and PE order.

**Figure 3** shows simulations of the longitudinal magnetization ( $M_z$ ) for WM and GM for varying number of phase steps (RF-pulses) per slice and two different flip angles. The figure illustrates the need for “dummy” slices to reach a steady value of longitudinal magnetization. More dummy slices are needed for lower flip angles and for lower number of phase steps per slice. Additionally, the actual value of magnetization reached depends on the number of phase steps per slice and appears to asymptotically approach true steady-state MT effects.

Overall, the simulations predicted the experimental results well. Our study assessed characteristic factors of the interslice MTR method to be considered for MTR imaging in the brain.

**References:** [1] Park, S.H. and Duong T.Q., Magn Reson Med, 2011. 65(6): p. 1702-10. [2] Graham, S.J. and Henkelman, R.M., J Magn Reson Imaging, 1997. 7(5):p. 903-12. [3] Stanisz, G.J., et al., Magn Reson Med, 2005. 54(3): p. 507-12.